

Blastemal Cells of Nephroblastomatosis Complex Share an Onco-Developmental Antigen with Embryonic Kidney and Wilms' Tumor

An Immunohistochemical Study on Polysialic Acid Distribution

JÜRGEN ROTH, MD, PhD, INGE BLAHA, MD,
DIETER BITTER-SUERMAN, MD,
and PHILIPP U. HEITZ, MD

From the Interdepartmental Electron Microscopy, Biocenter, University of Basle, Basle, the Institute of Pathology, University of Zürich, Zürich, Switzerland, the Department of Pathology, University of Mainz, Mainz, and the Institute of Medical Microbiology, Medical School, Hannover, Federal Republic of Germany

Previous investigations on polysialic acid of the neural cell adhesion molecule NCAM in human kidney have demonstrated its presence during nephrogenesis in embryonic kidney, absence in normal adult kidney, and reexpression in Wilms' tumor. These data showed that polysialic acid of NCAM is an onco-developmental antigen in human kidney and provided more direct evidence for the metanephric origin of Wilms' tumor. In the present study, five cases of Wilms' tumor associated with nephroblastomatosis complexes were immunohistochemically investigated with a monoclonal antibody for the presence of polysialic acid. Regardless of the type of nephroblastomatosis complex, ie, renal nodular blastema, simple tubular metanephric hamartoma, sclerosing metanephric hamartoma with ade-

noma, or incipient Wilms' tumor, immunoreactivity for polysialic acid was found in the blastemal cells, but was undetectable in all other structural elements. Because only blastemal cells exhibited a characteristic feature of embryonal differentiating metanephric derivatives, it appears that Wilms' tumor has its origin not exclusively in nodular renal blastema but rather in blastemal cells present in the various forms of nephroblastomatosis complex. The presence of polysialic acid of NCAM in blastemal cells in such lesions indicates that further events in addition to the expression of the embryonic form of this cell adhesion molecule may be involved in the pathogenesis of Wilms' tumor. (Am J Pathol 1988, 133:596-608)

WILMS' TUMOR (NEPHROBLASTOMA) is the most common malignant kidney tumor of childhood and is believed to derive from remnants of immature kidney tissue that have retained some features of the embryonic epoch of organ development.^{1,2} This widely accepted concept of metanephrogenic origin of Wilms' tumor is based on two different but causally related grounds. First, the histologic appearance of most Wilms' tumors is strikingly similar to structures found during the embryonic development of the metanephros.^{2,3} Under normal conditions, however, nephrogenesis ceases in the fetal human kidney 4-6

weeks before term and structures characteristic of the differentiation period are no longer found.⁴ The second observation in favor of the embryonic origin of Wilms' tumor is related to the fact that in at least one third of all Wilms' tumor-affected kidneys, foci of im-

Supported in part by grants from the Regionale Krebsliga beider Basel and the Swiss National Science Foundation to J. Roth and the Deutsche Forschungsgemeinschaft to D. Bitter-Suermann.

Accepted for publication August 4, 1988.

Address reprint requests to J. Roth, MD, PhD, Biocenter, University of Basle, CH-4056 Basle, Switzerland.

mature renal tissue of various morphologic appearances can be observed.⁵ These diffuse or multifocal lesions usually found in kidney cortex either adjacent to Wilms' tumor or in kidney regions uninvolved by tumor are now collectively comprised under the general term nephroblastomatosis complex.⁵⁻⁷ In their fundamental study, Bove and McAdams⁵ distinguished three types of nephroblastomatosis lesions that they considered to be neoplastic: 1) nodular renal blastema, 2) metanephric hamartoma, and 3) Wilms' tumorlet. The former and the latter were described as subcapsular, unencapsulated nodules composed of metanephric blastemal cells, the sole difference between them being their size. In contrast, metanephric hamartomas were described as highly variable in size and composed of congeries of primitive nephron segments embedded in a fibrocollagenous matrix. Besides simple forms, complex ones were distinguished that contained adenomas and incipient Wilms' tumor, ie, circumscribed monophasic proliferations of metanephric blastemal cells.

There is considerable interest in trying to define the biologic significance of these various, obviously inter-related lesions. Several lines of evidence suggest that nephroblastomatosis is an important factor that appears to be associated with the development of Wilms' tumor and may be considered a premalignant lesion.⁵⁻⁸ It was hypothesized that classic Wilms' tumor arises in a hamartomatous metanephric precursor, which in turn originated in late gestation from a nodular renal blastema. But metanephric hamartoma frequently display signs of regression and there is morphologic and clinical evidence that they not necessarily give rise to Wilms' tumor.⁵⁻¹⁰ Bove and McAdams⁵ have speculated that Wilms' tumor development represents an example for the "two hit" theory of carcinogenesis.^{11,12} A first mutational event would lead to a benign aberrant metanephric proliferation, ie, nephroblastomatosis complex, which would provide the substrate for tumor development after a second post-natal mutational event.

We have recently shown that the long-chain form of polysialic acid present on the neural cell adhesion molecule is present during certain differentiation stages of metanephron development in rat¹³ and human¹⁴ kidney. These observations prompted further investigations on Wilms' tumor that demonstrated the presence of such units of polysialic acid in the various histologic forms of Wilms' tumor.^{14,15} Further, they proved the absence of polysialic acid in fully differentiated, normal human kidney.^{14,15} Collectively, these observations led us to conclude that the long-chain form of polysialic acid, characteristic of the weakly adhesive form of NCAM, represents an

onco-developmental antigen in human kidney. The demonstration of a molecule characteristically expressed during nephrogenesis but absent after its cessation provided new information supporting the concept of metanephric origin of Wilms' tumor. In the present study, five cases of Wilms' tumor that were found to be associated with various forms of nephroblastomatosis complexes were immunohistochemically investigated with a monoclonal antibody for possible presence of polysialic acid.

Materials and Methods

Reagents

The mouse monoclonal IgG2a antibody MAb 735 raised against live group B meningococci was used to detect homopolymers of α 2,8 linked N-acetylneuraminic acid (polysialic acid). Production and characterization of the antibody were described in detail.¹⁶ The monoclonal antibody requires the presence of at least eight α 2,8 linked N-acetylneuraminic acid residues for binding^{13,17} and has no crossreactivity with polynucleotides and denatured DNA (manuscript in preparation). Two bacteriophage encoded endosialidases specifically hydrolyzing α 2,8 linked N-acetylneuraminic acid were used: 1) bacteriophage PK1A-bound endosialidase,¹⁸ and 2) soluble, purified bacteriophage E-encoded endosialidase.¹⁹ Bacteriophage PK1A-bound endosialidase has a reported strict substrate specificity: it requires the presence of at least eight α 2,8 linked N-acetylneuraminic acid residues for cleavage.¹⁸ Protein A-gold complexes were prepared with 8 or 14 nm gold particles as reported in detail elsewhere.^{20,21} Staphylococcal protein A was purchased from Pharmacia Fine Chemicals (Uppsala, Sweden), affinity-purified rabbit anti-mouse IgG (heavy and light chain) from Cappel Laboratories (West Chester, PA), colominic acid (sodium salt) and bovine serum albumin from Sigma (St. Louis, MO), Carbowax 20M, hydroquinone and silver lactate from Fluka (Buchs, Switzerland), and tetrachloroauric acid and trisodium citrate from Merck (Darmstadt, FRG). All other reagents were of highest available purity.

Tissue Fixation and Embedding

Tissue pieces from surgically removed kidneys were routinely fixed in 10% phosphate-buffered formaldehyde and embedded in paraffin according to standard procedures. From each tumor two to five different regions and adjacent normal kidney were embedded.

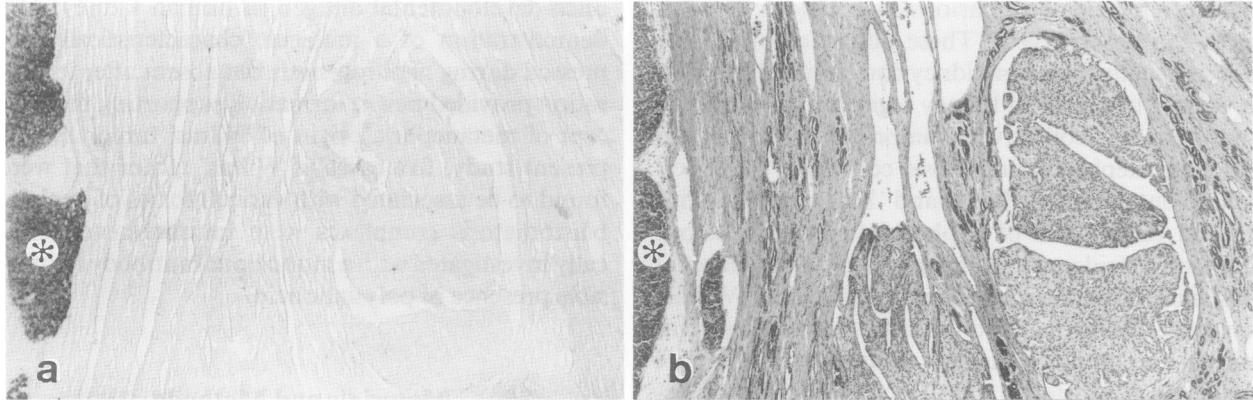


Figure 1—Immunohistochemical demonstration of polysialic acid with the protein A-gold technique. Due to photochemical silver amplification of the gold particle label, positive immunostaining is seen in black in all micrographs. **a**—Part of a strongly polysialic acid positive, monomorphic Wilms' tumor (asterisk) and the adjacent negative sclerosing metanephric hamartoma with adenoma are shown. **b**—Section adjacent to A stained with H&E. a and b, $\times 30$

Immunohistochemistry

Paraffin sections (5μ) mounted on glass slides were deparaffinized and rehydrated. Before incubation with antibodies the sections were covered with 0.5% ovalbumin or 4% defatted milk powder dissolved in phosphate-buffered saline (PBS) (10 mM phosphate buffer, pH 7.2) for 5 minutes.

Immunoreactive sites for polysialic acid were detected with the protein A-gold technique^{20,21} followed by photochemical silver amplification^{22,23} as detailed previously.^{13,14} Monoclonal anti-polysialic acid antibody was used at 500-fold dilution followed by 25 or 50 μ g/ml affinity-purified rabbit anti-mouse IgG, both of them diluted with PBS containing either 1% BSA and 0.075% Triton X-100 and Tween 20 or 2% defat-

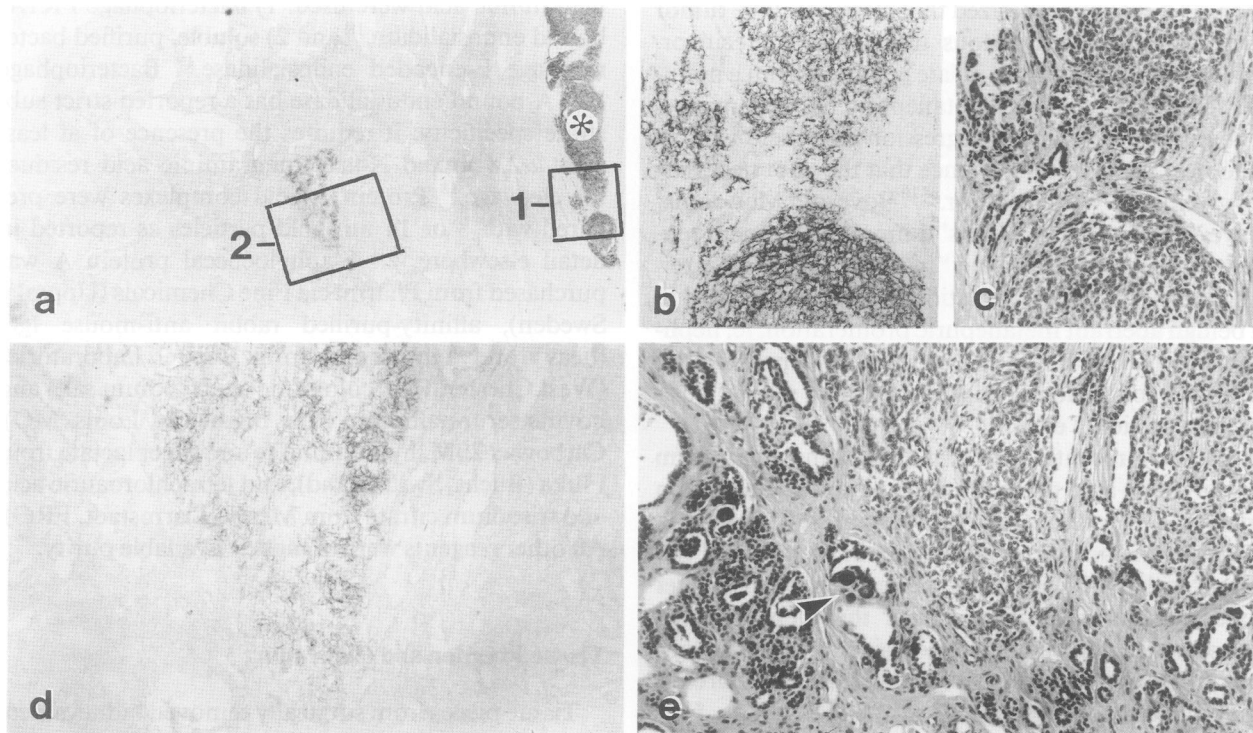


Figure 2a—Low-power micrograph showing part of a polysialic acid positive blastemal Wilms' tumor (asterisk) and an adjacent unstained sclerosing metanephric hamartoma with adenoma. **b**—Detail (marked square 1 in a) from the peripheral region of the positive Wilms' tumor. **c**—Section adjacent to b stained with H&E. In the hamartoma, a nest of polysialic acid positive cells exist (marked square 2 in a) that is shown at higher magnification in **d**. **e**—Section adjacent to d stained with H&E. Note the numerous small tubules and immature glomeruli as well as psammom bodies (arrowhead) in the neighborhood of the blastemal cells that are not stained for polysialic acid in d. a, $\times 55$; b-e, $\times 100$

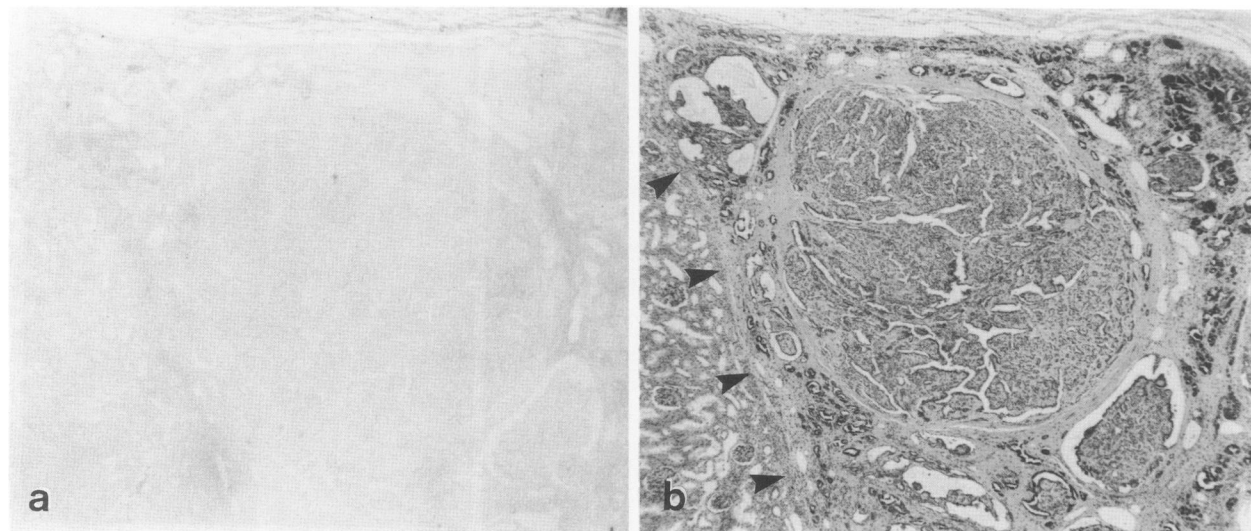


Figure 3a—Polysialic acid negative sclerosing metanephric hamartoma with adenoma. The adjacent normal kidney parenchyma is also not stained. **b**—Section adjacent to a stained with H&E. The border between the hamartoma and the normal kidney parenchyma is indicated by arrowheads. a,b, $\times 20$

ted milk powder. Protein A-gold was used at $OD_{525\text{ nm}} = 0.7$ diluted with PBS containing 1% BSA and 0.075% Triton X-100 and Tween 20. Duration of photochemical silver amplification was approximately 3 minutes. Finally, the sections were dehydrated through graded alcohol, cleared with xylene and mounted with Canada balsam. Sometimes sections were stained with Kernechtrot after immunostaining.

The following specificity tests were performed: 1) omission of the monoclonal antibody, 2) omission of both primary and secondary antibody, 3) preabsorption of the monoclonal antibody with colominic acid (*Escherichia coli* K1 capsular polysaccharide composed of homopolymers of $\alpha 2,8$ linked N-acetylneuraminic acid), 4) substitution of the monoclonal anti-polysialic acid antibody by various unrelated mouse monoclonal antibodies, and 5) digestion of tissue sections before immunolabeling with PK1A endosialidase (10^9 pfu/ml, 2 or 17 hours at 37 C) or with endosialidase E ($10\ \mu\text{g}/\text{ml}$ for 40 minutes, or 50 or 200 $\mu\text{g}/\text{ml}$ for 20 minutes at 37 C).

Case Reports and Results

Case 1

Resected kidney from a 4.6-year-old girl containing one tumor measuring approximately 10 cm in diameter and two smaller tumors, 3.5 cm and 2.5 cm, which were separated from each other and the large tumor by normal-appearing kidney parenchyma, was studied.

Histologically, the large tumor consisted of blastemal masses, sequestered by delicate fibrous septa, showing moderate signs of differentiation in the form of palisades. The entire tumor with the exception of the septa was intensely positive for polysialic acid. In subcapsular regions adjacent to the tumor a sclerosing hamartoma with central adenomas and numerous cystic lymphatics and psammoma bodies was found. No immunostaining for polysialic acid was detectable in these structures (Figure 1). A small region inside this lesion, however, consisted of a nest of cells that exhibited positive, albeit weak, cell surface staining for polysialic acid (Figure 2a, d). These cells were reminiscent of blastemal cells (Figure 2e). The adjacent normal kidney tissue was immunohistochemically negative for polysialic acid.

The tumor measuring 3.5 cm in diameter consisted exclusively of strongly polysialic acid positive blastemal masses that exhibited focal palisade formation. A sclerosing metanephric hamartoma with papillary adenomas, small cysts lined by flat epithelium and numerous psammoma bodies was found in its periphery and exhibited no immunostaining for polysialic acid (Figure 3).

The third tumor was of biphasic character with blastemal cell masses showing epithelial differentiation, ie, palisade and tubule formation. All these structures exhibited immunostaining for polysialic acid. A sclerosing metanephric hamartoma with adenomas found adjacent to it exhibited no immunostaining for polysialic acid.

Case 2

Resected kidney from a 1.5-year-old boy with a tumor measuring 6 cm in diameter and two others, 3.5

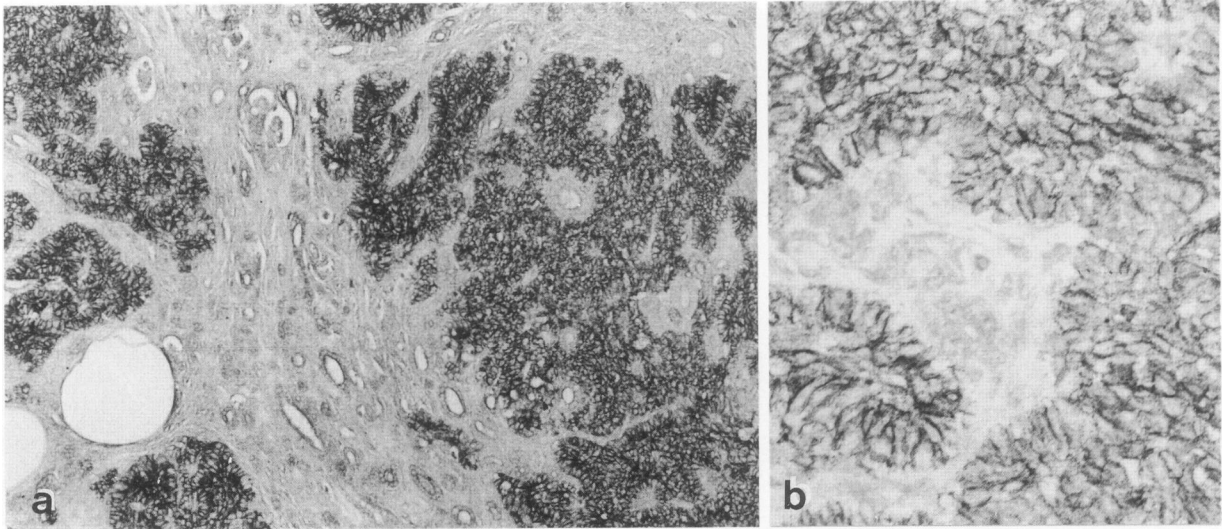


Figure 4a—Triphasic Wilms' tumor exhibiting immunostaining for polysialic acid over the blastema, glomeruloid bodies and tubules. **b**—Higher magnification showing positive blastema and negative stroma. a, $\times 70$; b, $\times 300$

cm and 1.5 cm, which were separated from each other and the larger tumor by macroscopically normal-appearing kidney parenchyma was studied. A metastasis was detected in a hilar lymph node.

Histologically, the large tumor exhibited the features of a classical triphasic Wilms' tumor with intensely polysialic acid positive blastemal masses. Glomeruloid bodies and tubules were also positive but showed considerable variability in intensity of immunostaining. The stroma did not stain for polysialic acid (Figure 4).

The larger of the two other tumors was histologically dominated by a papillary adenoma that was immunohistochemically negative for polysialic acid; however, some microscopic foci of polysialic acid positive blastemal cells sometimes forming palisades existed within this adenoma (Figure 5). Glomeruloid bodies occasionally were seen in sites that did not stain for polysialic acid. In the vicinity of this adenoma, a predominantly sclerosing metanephric hamartoma that also contained small tubules and abortive glomeruli was observed. None of these structures was positive for polysialic acid; however, some microscopic nests of polysialic acid positive blastemal cells existed here. On examination of serial sections, a few small adenomas, which were not stained for polysialic acid, were found in this hamartoma. Examination of subcapsular regions of the adjacent kidney tissue revealed the presence of numerous immature and sclerosing glomeruli as well as some foci of mild interstitial lymphocytic infiltrates. This region as well as the normal-appearing adjacent cortex and medulla were immunohistochemically negative for polysialic acid.

The subcapsular tumor measuring 1.5 cm in diameter exhibited triphasic character with strongly polysialic acid positive blastemal nests as well as positive tubules and glomeruloid bodies. The stroma exhibited no immunostaining for polysialic acid. Adjacent to it, a sclerosing metanephric hamartoma with a few, small adenomas and cysts together with immature glomeruli was found (Figure 6). The cuboidal cells lining the cysts exhibited immunostaining for polysialic acid at varying degree (Figure 6a, b). Blastemal nests, often composed of only a few cells, were positive (Figure 6c, d). No immunostaining for polysialic acid was associated with the immature glomeruli and tubules (Figure 6c), the adenomas (Figure 6b), and the stroma. Inspection of subcapsular regions adjacent to the lesion revealed the presence of immature, polysialic acid-negative glomeruli.

Case 3

Resected kidney from a 3.75-year-old girl was studied. The kidney was almost completely replaced by tumor masses. Tumor invasion of blood vessels, of the renal capsule and the adipose tissue was macroscopically evident.

Histologically, the entire tumor was composed of polysialic acid positive blastema separated by delicate not immunostained fibrous septa. Tumor invasion of adjacent kidney tissue and renal veins often was observed. Examination of the adjacent tissue revealed fibrous thickening of the renal capsule and the presence of a simple tubular metanephric hamartoma composed of small tubules lined by cuboidal cells with

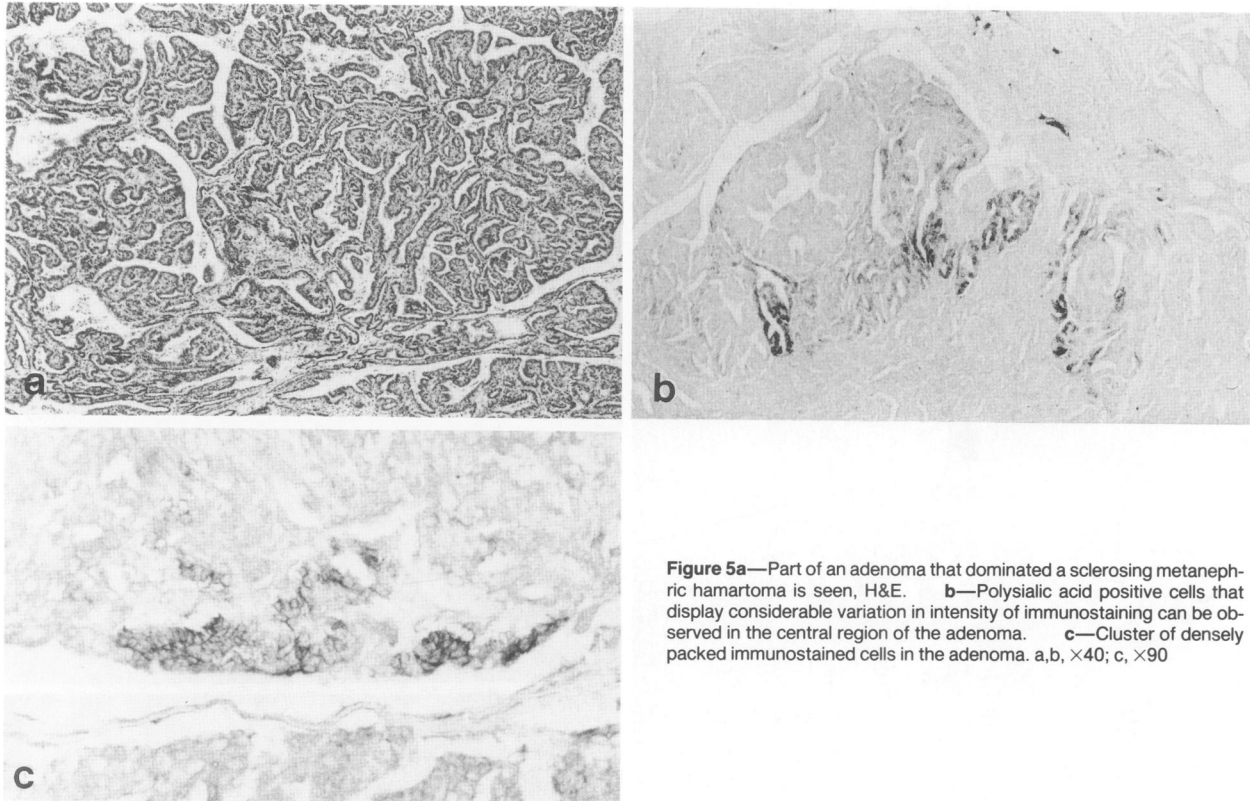


Figure 5a—Part of an adenoma that dominated a sclerosing metanephric hamartoma is seen, H&E. **b**—Polysialic acid positive cells that display considerable variation in intensity of immunostaining can be observed in the central region of the adenoma. **c**—Cluster of densely packed immunostained cells in the adenoma. a,b, $\times 40$; c, $\times 90$

hyperchromatic nuclei, a few abortive immature glomeruli, and occasionally microscopic blastemal cell nests embedded in a fibrocollagenous matrix (Figure 7b). This lesion was separated from the Wilms' tumor by normal tissue. Only the blastemal cell nests exhibited weak immunostaining for polysialic acid, whereas the tubules and immature glomeruli present in the hamartoma were unstained (Figure 7a).

Case 4

Resected kidney from a 1.75-year-old boy containing a tumor approximately 6.5 cm in diameter and numerous smaller, 1–2.5 cm tumors separated from the larger tumor by normal-appearing kidney was studied.

Histologically, the main tumor was a strongly polysialic acid positive, monomorphous, undifferentiated blastemal Wilms' tumor exhibiting focally epithelial differentiations, ie, palisades and small tubules.

Investigation of a tumor approximately 2 cm in diameter revealed two characteristic components that were so heavily interwoven that they seemed to represent a single entity. One component consisted of polysialic acid-positive blastemal cell masses (Figure 8a). The other component was represented by many broad fibrocollagenous bands that contained groups of small

tubules, immature glomeruli, and variably sized blastemal cell nests, all typical features of a simple tubular metanephric hamartoma (Figure 8b). Only the blastemal cell component and immature tubular cells were positive for polysialic acid (Figure 8a).

Another small tumor represented similar albeit slightly different features (Figure 9). It was composed predominantly of structures characteristic of a simple tubular metanephric hamartoma in which blastemal nests of variable size and shape were a prominent element (Figure 10). This lesion as a whole formed a well-demarcated nodule, however, although no separating fibrous capsule existed at the border region to normal kidney. Further, one internal, purely blastemal mass exhibiting epithelial differentiations formed a large, circumscribed nodule (Figures 9a and 10c, d). All blastemal elements were strongly positive for polysialic acid. The tubules and immature glomeruli as well as the surrounding normal kidney were not stained.

Case 5

Resected kidney from a 1.75-year-old boy with a large tumor mass and two 2.5 and 1.5 cm subcapsular tumors was studied.

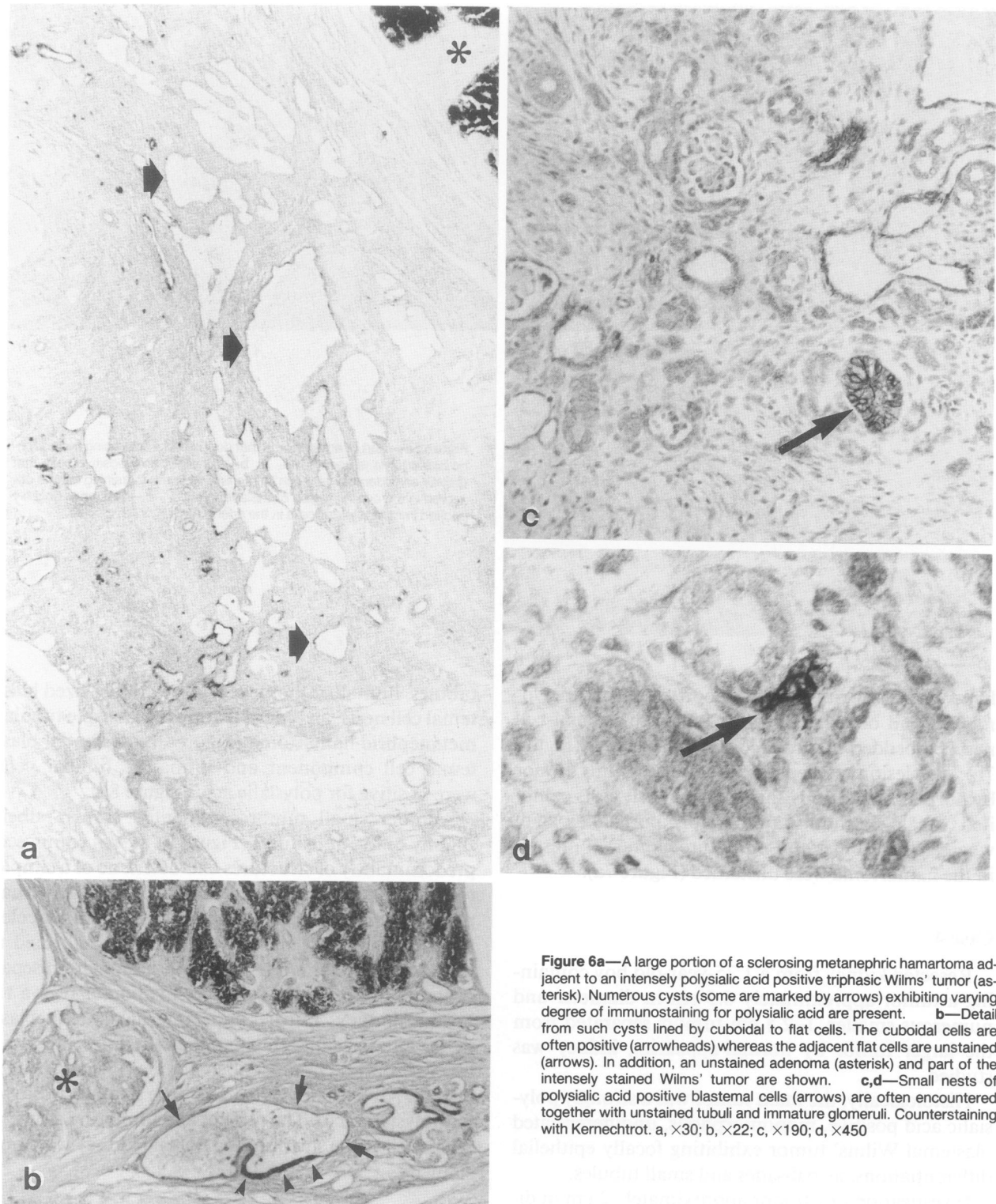


Figure 6a—A large portion of a sclerosing metanephric hamartoma adjacent to an intensely polysialic acid positive triphasic Wilms' tumor (asterisk). Numerous cysts (some are marked by arrows) exhibiting varying degree of immunostaining for polysialic acid are present. **b**—Detail from such cysts lined by cuboidal to flat cells. The cuboidal cells are often positive (arrowheads) whereas the adjacent flat cells are unstained (arrows). In addition, an unstained adenoma (asterisk) and part of the intensely stained Wilms' tumor are shown. **c,d**—Small nests of polysialic acid positive blastemal cells (arrows) are often encountered together with unstained tubuli and immature glomeruli. Counterstaining with Kernechtrot. a, $\times 30$; b, $\times 22$; c, $\times 190$; d, $\times 450$

Histologically, the main tumor was a polysialic acid positive typical triphasic Wilms' tumor. The two smaller tumors were of monomorphous blastemal character, whereby the smaller of the two showed epithelial differentiations (Figure 11c, d). Both were im-

munohistochemically positive for polysialic acid. The adjacent normal kidney tissue showed signs of compression. In subcapsular regions of the adjacent normal kidney parenchyma, nodular renal blastemas of varying sizes were detectable that occasionally con-

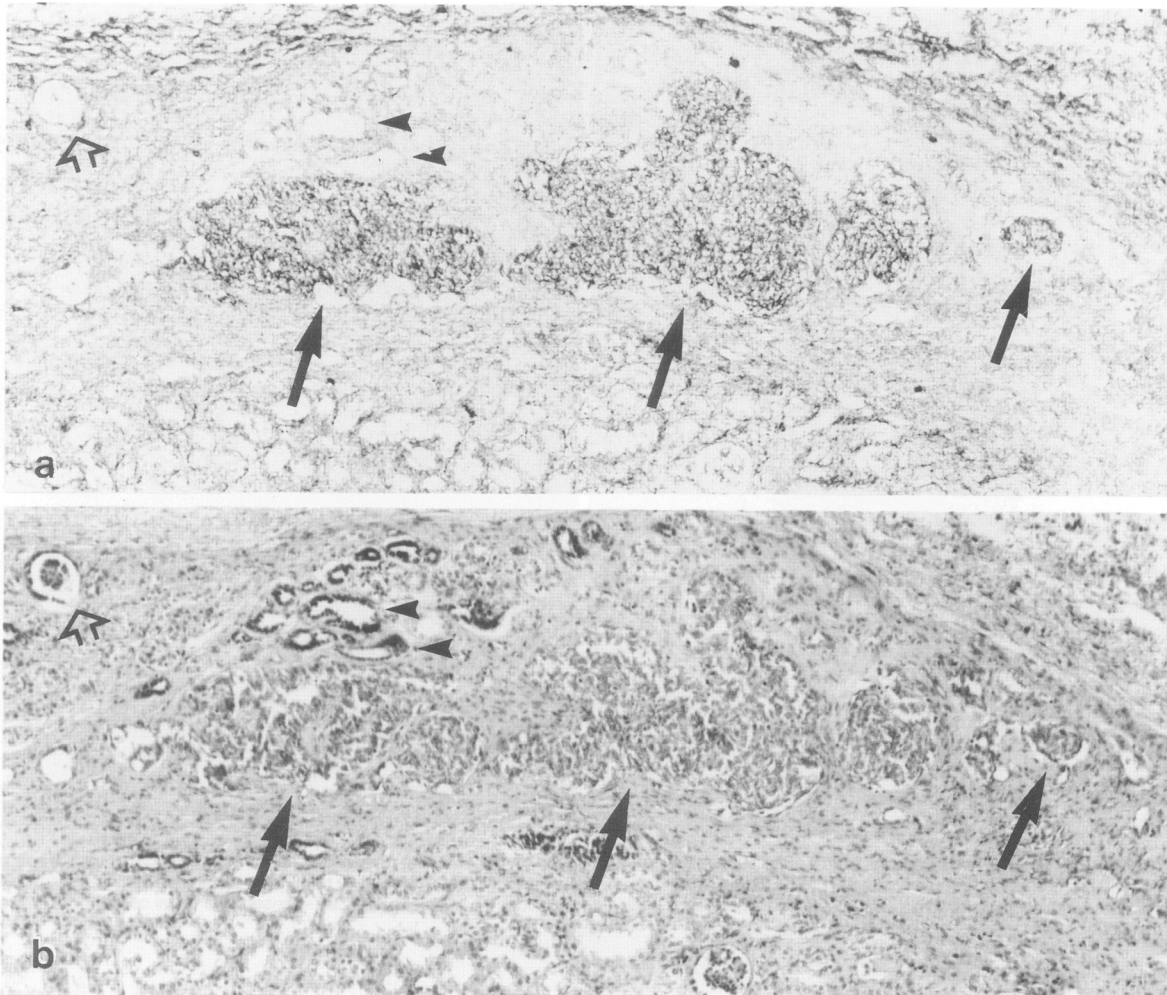


Figure 7a—Portion of a simple tubular metanephric hamartoma that exhibits small nests of polysialic acid positive blastemal cells (arrows). Tubules (arrowheads) and immature glomeruli (open arrow) are not stained. **b**—Section adjacent to a stained with H&E. a,b, $\times 85$

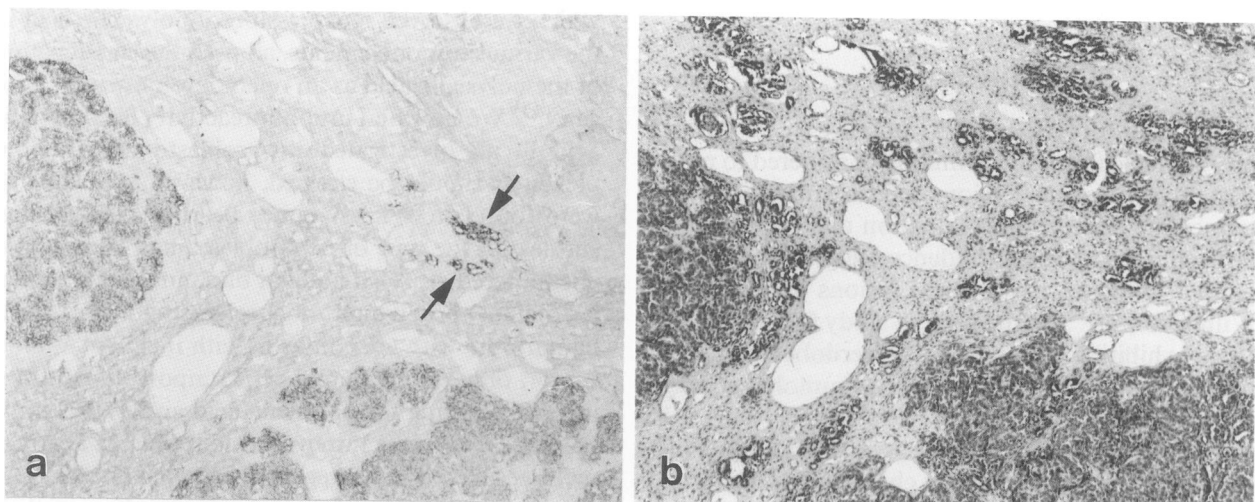


Figure 8a—Part of a predominantly monomorphic blastemal Wilms' tumor in which the intimate relationship between large polysialic acid positive blastemal cell masses and the simple tubular metanephric hamartoma can be appreciated. Some polysialic acid positive immature tubular cells are present in the hamartoma (arrows). **b**—Section adjacent to a stained with H&E. a,b, $\times 50$

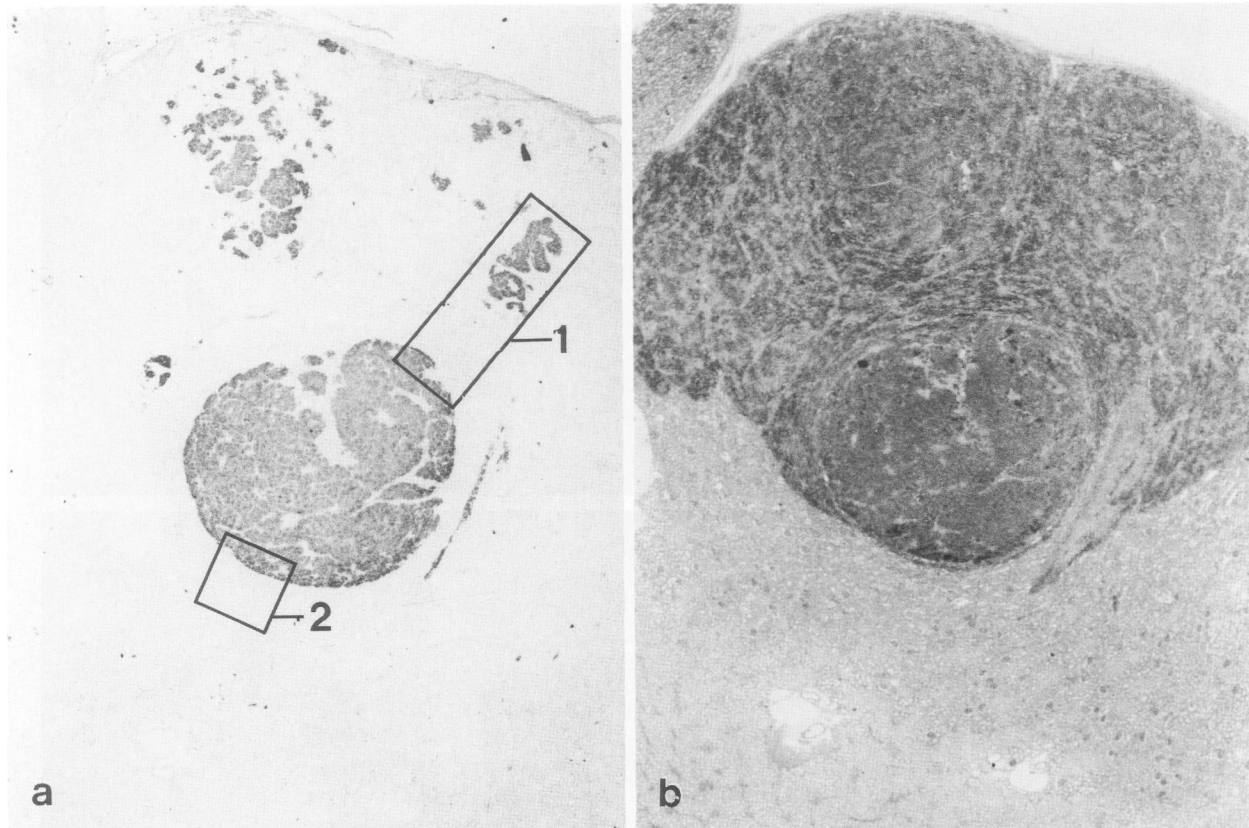


Figure 9—Two consecutive serial sections from a small subcapsular tumor. **a**—Immunostaining reveals that only a well-demarcated nodule contained in the tumor and some smaller, irregularly shaped cell nests are positive for polysialic acid. Regions marked by rectangles are shown at higher magnification in Figure 10. The remainder of the tumor is as unstained as the surrounding normal kidney parenchyma. **b**—Consecutive serial section to a stained with H&E. a,b, $\times 30$

tained immature glomeruli. The nests of blastemal cells were positive for polysialic acid (Figure 11a); however, the immature glomeruli were not immunostained.

Discussion

The nephroblastomatosis complex in its various morphologic forms is commonly considered to represent a dysontogenetic lesion of the infantile kidney intermediate between malformation and neoplasm. In fact, clinicopathologic evidence suggests a potential premalignant nature of these lesions giving rise to Wilms' tumor.⁵⁻⁹ In the present study five Wilms' tumors exhibiting intralobular or perilobular nephroblastomatosis complexes were immunohistochemically investigated for the presence of polysialic acid with a monoclonal antibody recognizing the long-chain form of this polyglycan characteristically found on the weakly adhesive embryonic form of the neural cell adhesion molecule NCAM. The rationale for this study was our initial observation that such polysialic

acid units represented a developmentally regulated antigen in differentiating rat and human kidney that was no longer expressed after cessation of nephrogenesis.^{13,14} Subsequent studies on Wilms' tumor, in which we observed reexpression of polysialic acid in the various tumor elements, allowed the classification of the polysialic acid as an onco-developmental antigen.^{14,15} We now find immunoreactivity for polysialic acid in all investigated nephroblastomatosis complexes. It should be stressed, however, that they all were found in Wilms' tumor-bearing kidneys. Regardless of the type of nephroblastomatosis complex encountered, ie, renal nodular blastema, simple tubular metanephric hamartoma, sclerosing metanephric hamartoma with adenomas or with incipient Wilms' tumor, only the blastemal cell component exhibited immunostaining for polysialic acid and occasionally observed structures interpreted to represent aberrant renal vesicles. The aggregates of blastemal cells were always positive for polysialic acid regardless of their size. Even the smallest blastemal nests could exhibit intensity of immunostaining equivalent to that ob-

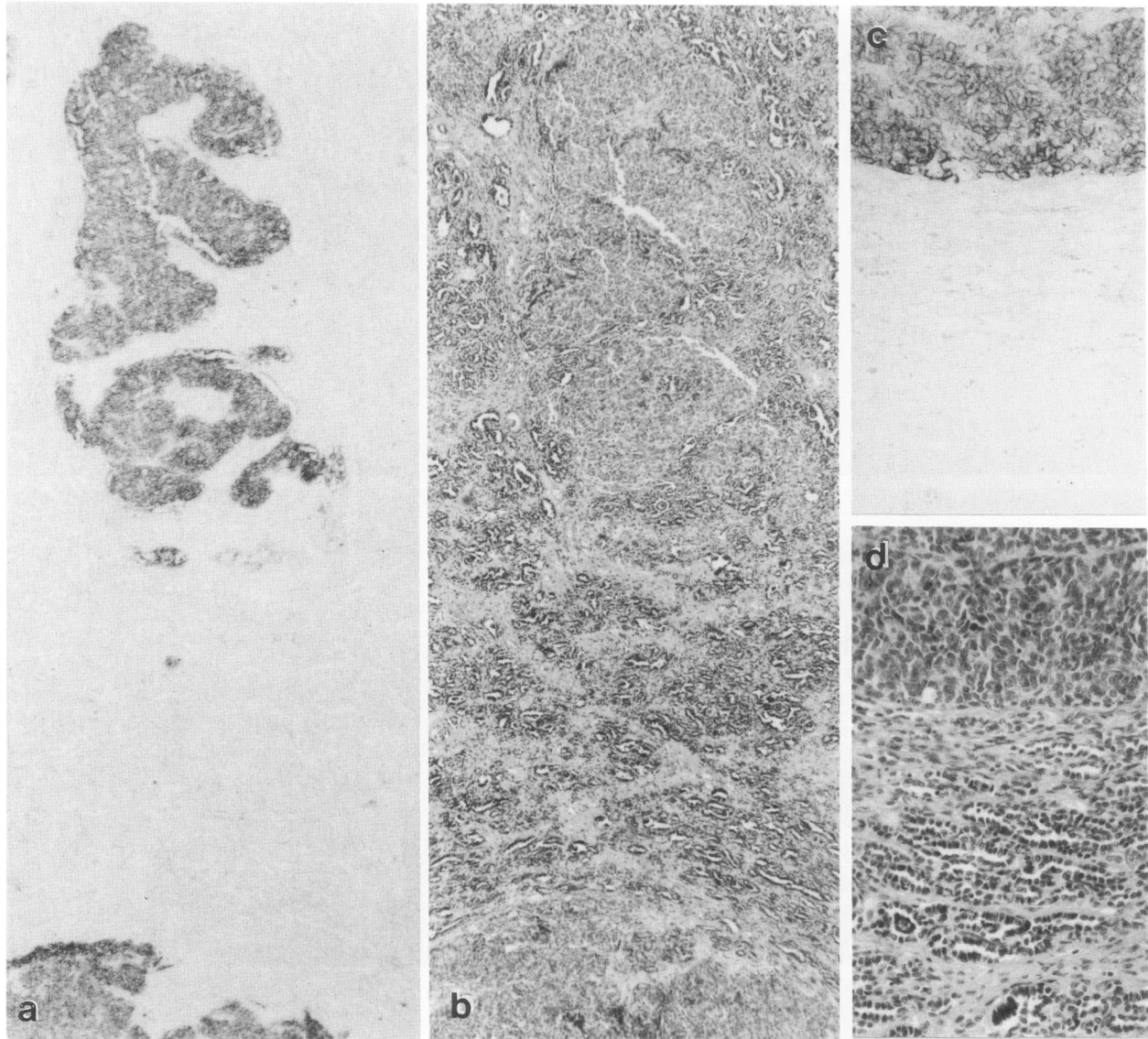


Figure 10a—Detail 1 from Figure 9a showing an irregularly shaped nest of polysialic acid positive blastemal cells surrounded by unstained simple tubular hamartoma. **b**—Consecutive serial section to a stained with H&E. **c**—Detail 2 from Figure 9a showing the periphery of the intensely stained nodule that is composed of blastemal cells. The adjacent simple tubular metanephric hamartoma is polysialic acid negative. **d**—Consecutive serial section to c stained with H&E. a,d, $\times 58$

served in an adjacent Wilms' tumor. Consequently, it can be concluded that in nephroblastomatosis complexes only these cells have retained a feature characteristic of differentiation-competent blastemal cells present in embryonic human kidney. Although primitive tubules of S-shaped bodies or early capillary loop stages during normal metanephros development in embryonic human kidney and in Wilms' tumor were found to be positive for polysialic acid, those present in the nephroblastomatosis complexes were not positive. Obviously one has to wonder what biologic relevance these observations bear on the genesis of Wilms' tumor. Bove and McAdam^{5,24} speculated that

all nephroblastic tumors arise from nodular renal blastema either directly or indirectly by way of the development of a complex metanephric hamartoma. They specifically considered proliferating blastemal cells within a complex metanephric hamartoma as remnants of nodular renal blastema from which the hamartoma had derived. The present observation of small, polysialic acid-positive blastemal cell aggregates in simple tubular metanephric hamartoma that may eventually proliferate, as does nodular renal blastema, lends support to the speculation that Wilms' tumor may primarily arise from both lesions. This is not to exclude the possibility that the transforming poten-

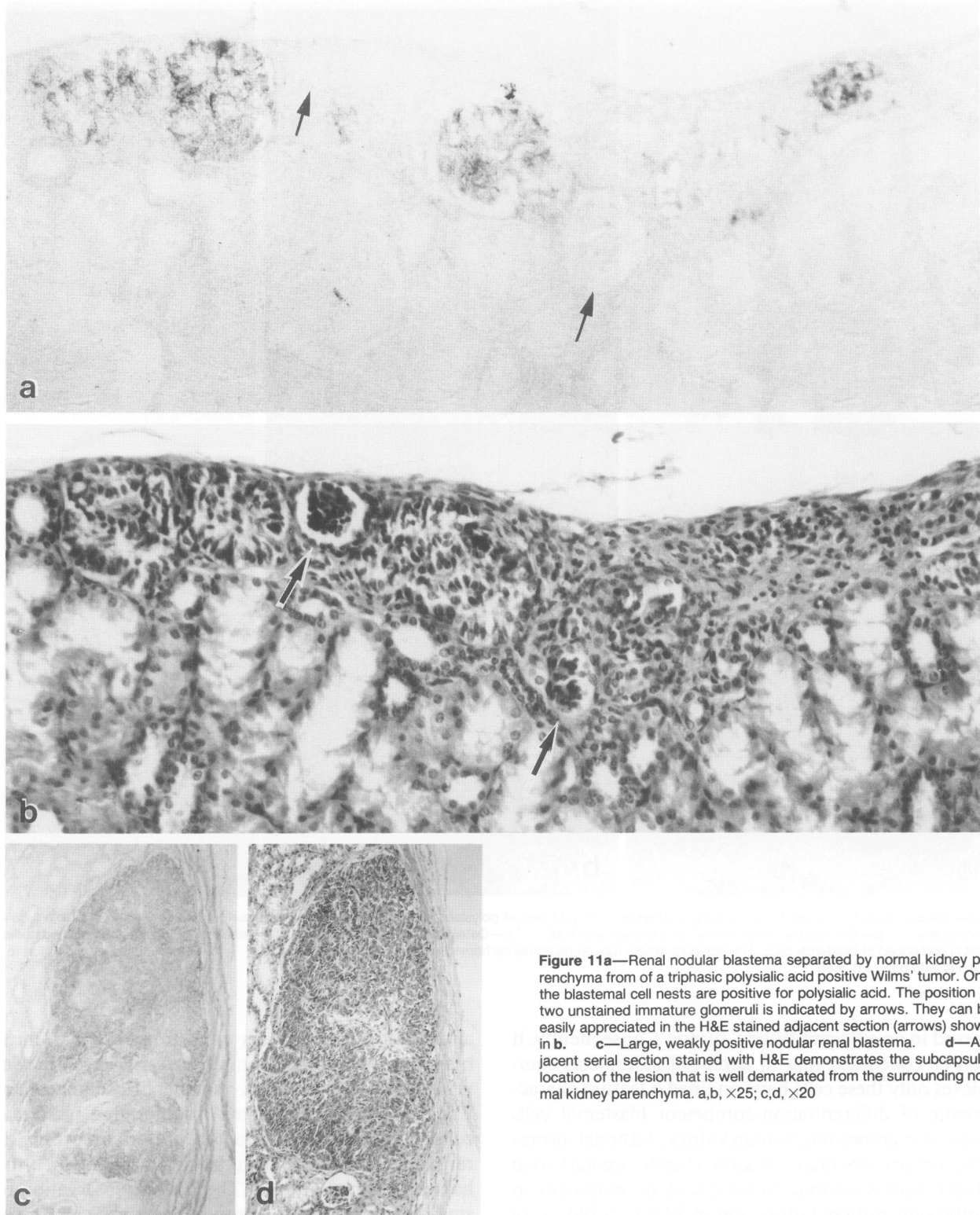


Figure 11a—Renal nodular blastema separated by normal kidney parenchyma from a triphasic polysialic acid positive Wilms' tumor. Only the blastemal cell nests are positive for polysialic acid. The position of two unstained immature glomeruli is indicated by arrows. They can be easily appreciated in the H&E stained adjacent section (arrows) shown in **b**. **c**—Large, weakly positive nodular renal blastema. **d**—Adjacent serial section stained with H&E demonstrates the subcapsular location of the lesion that is well demarcated from the surrounding normal kidney parenchyma. a,b, $\times 25$; c,d, $\times 20$

tial of blastemal cells present in a nodular renal blastema may be different from those in a metanephric hamartoma. In view of the present observations however, it seems justified to assume that the cellular ori-

gin of Wilms' tumors is from blastemal cells irrespective of the type of nephroblastomatosis complex. Because the tubules and glomeruloid bodies present in Wilms' tumor are positive for polysialic acid, in con-

trast to the one observed in metanephric hamartoma, they might derive from malignant blastemal cells. This assumption is further substantiated by the presence of polysialic acid-positive S-shaped bodies in Wilms' tumor.¹⁵

The persistence of cell surface polysialic acid in blastemal cells of nephroblastomatosis complexes in the kidney years after birth indicates that additional events must take place to realize the malignant cell phenotype, in accordance with the "two hit" theory of carcinogenesis.^{11,12} Wilms' tumor has been correlated with the constitutional deletion of chromosomal band 11p13.^{24,25} It is important to note that chromosome 11 encodes several genes associated with growth, development, and cancer,²⁶ among them the NCAM gene located on 11q23.²⁷ Specifically, the p15 and p13 regions encode growth factors, hormones, or both that can stimulate cell proliferation, whereas the q13 and q23 regions are fragile sites thought to be associated with cancer chromosome breakage. Insulinlike growth factor-2, an embryonal mitogen, was located on the 11p14/15 band that coincides with the location of the structural gene for insulin^{28,29} and is in the immediate vicinity of the Wilms' tumor gene. Recent investigations have provided clear evidence for the expression of insulinlike growth factor-2 gene not only in embryonic kidney but also in Wilms' tumor.^{29,30} It was markedly increased relative to adult kidney in both cases, however, the genes coding for insulinlike growth factor-1, insulin, and calcitonin, which are also located on chromosome 11, were not expressed in Wilms' tumor or in embryonic or normal adult kidney.³⁰ Furthermore, in the same study comparable low levels of c-H-ras-1 mRNA were found in normal kidney and Wilms' tumor. Low levels of α -TGF mRNA were present in some Wilms' tumors, but none in embryonic kidney. Analysis of N-myc gene levels in human kidney showed expression in embryonic but almost none in adult kidney and greatly enhanced expression in Wilms' tumor.³¹⁻³³ These results indicate that a number of molecular mechanisms may be important in the pathogenesis of Wilms' tumor. Expression of proto-oncogenes, autocrine growth factors, and a cell adhesion molecule may provide the basis for the selected persistence or expression of a less differentiated developmental state where growth regulation is less stringent. Studies are now in progress to investigate insulinlike growth factor-2 and N-myc mRNA by *in situ* hybridization techniques in nephroblastomatosis complex compared with embryonic kidney and Wilms' tumor.

References

1. Gonzalez-Crussi F: The pathology of Wilms' tumor, Wilms' Tumor (Nephroblastoma) and Related Renal

- Neoplasms of Childhood. Edited by F. Gonzalez-Crussi. Boca Raton, FL, CRC Press, 1984, pp 177-206
2. Mierau GW, Beckwith JB, Weeks DA: Ultrastructure and histogenesis of the renal tumors of childhood: An overview. *Ultrastruct Pathol* 1987, 11:313-333
3. Schmidt D, Dickersin GR, Vawter GF, Mackay B, Harms D: Wilms' tumor: Review of ultrastructure and histogenesis. *Pathobiol Ann* 1982, 12:281-300
4. Saxen L: Organogenesis of the kidney, *Developmental and Cell Biology Series*. Edited by PW Barlow, PB Green, CC Wylie. Cambridge, Cambridge University Press, 1987, 19:1-173
5. Bove KE, McAdams AJ: The nephroblastomatosis complex and its relationship to Wilms' tumor: A clinicopathologic treatise. *Persp Paed Path* 1976, 3:185-222
6. Machin GA: Persistent renal blastema (nephroblastomatosis) as a frequent precursor of Wilms' tumor, a pathological and clinical review. Part 1. Nephroblastomatosis in context of embryology and genetics. *Am J Pediatr Hematol Oncol* 1980, 2:165-171
7. Machin GA: Persistent renal blastema (nephroblastomatosis) as a frequent precursor of Wilms' tumor, a pathological and clinical review. Part 2. Significance of nephroblastomatosis in the genesis of Wilms' tumor. *Am J Pediatr Hematol Oncol* 1980, 2:253-261
8. Machin GA: Persistent renal blastema (nephroblastomatosis) as a frequent precursor of Wilms' tumor, a pathological and clinical review. Part 3. Clinical aspects of nephroblastomatosis. *Am J Pediatr Hematol Oncol* 1980, 2:353-362
9. Heideman RL, Haase GM, Foley CL, Wilson HL, Bailey WC: Nephroblastomatosis and Wilms' tumor. *Cancer* 1985, 55:1446-1451
10. De Chadarevian J-P, Fletcher BD, Chatten J, Rabino-vitch HH: Massive infantile nephroblastomatosis: A clinical, radiological, and pathological analysis of four cases. *Cancer* 1977, 39:2294-2305
11. Ashley DJB: The "two hit" and "multiple hit" theories of carcinogenesis. *Br J Cancer* 1969, 23:313-328
12. Knudson A, Strong LJ: Mutation and cancer: A model for Wilms' tumor of the kidney. *J Natl Cancer Inst* 1972, 48:313-328
13. Roth J, Taatjes DJ, Bitter-Suermann D, Finne J: Polysialic acid units are spatially and temporally expressed in developing postnatal rat kidney. *Proc Natl Acad Sci USA* 1987, 84:1969-1973
14. Roth J, Wagner P, Zuber C, Weisgerber C, Heitz PU, Goridis C, Bitter-Suermann D: Reexpression of polysialic acid units of the neural cell adhesion molecule in Wilms' tumor. *Proc Natl Acad Sci USA* 1988, 85:2999-3003
15. Roth J, Zuber C, Wagner P, Blaha I, Bitter-Suermann D, Heitz PU: Presence of the long chain form of polysialic acid of the neural cell adhesion molecule in Wilms' tumor: Identification of a cell adhesion molecule as an onco-developmental antigen and implications for tumor histogenesis. *Am J Pathol* 1988, 133:227-240
16. Frosch M, G6rgen I, Boulnois GJ, Timmis KN, Bitter-Suermann D: NZB mouse system for production of monoclonal antibodies to weak bacterial antigens: Isolation of an IgG antibody to the polysaccharide capsules of *Escherichia coli* K1 and group B meningococci. *Proc Natl Acad Sci USA* 1985, 82:1194-1198

17. Finne J, Bitter-Suermann D, Goridis C, Finne U: An IgG monoclonal antibody to group B meningococci crossreacts with developmentally regulated polysialic acid units of glycoproteins in neural and extraneural tissues. *J Immunol* 1987, 138:4402-4407
18. Finne J, Mäkela PH: Cleavage of the polysialosyl units of brain glycoproteins by a bacteriophage endosialidase. Involvement of a long oligosaccharide segment in molecular interactions of polysialic acid. *J Biol Chem* 1985, 260:1265-1270
19. Tomlinson S, Taylor PW: Neuraminidase associated with coliphage E that specifically depolymerizes the Escherichia coli K1 capsular polysaccharide. *J Virol* 1985, 55:374-378
20. Roth J, Bendayan M, Orci L: Ultrastructural localization of intracellular antigens by the use of protein A-gold complex. *J Histochem Cytochem* 1978, 26:1074-1081
21. Roth J: The protein A-gold technique—A qualitative and quantitative approach for antigen localization in thin sections, *Techniques in Immunocytochemistry*. Edited by GL Bullock, P Petrusz. London, Academic Press, 1982, 1:107-133
22. Manigley C, Roth J: Applications of immunocolloids in light microscopy. IV. Use of photochemical silver staining in a simple and efficient double-staining technique. *J Histochem Cytochem* 1985, 33:1247-1253
23. Taatjes DJ, Schaub U, Roth J: Light microscopical detection of antigens and lectin binding sites with gold-labelled reagents on semi-thin Lowicryl K4M sections: Usefulness of the photochemical silver reaction for signal amplification. *Histochem J* 1987, 19:235-245
24. Riccardi VM, Sujansky E, Smith AC, Francke U: Chromosomal imbalance in the aniridia-Wilms' tumor association: 11p interstitial deletion. *Pediatrics* 1978, 61:604-610
25. Francke U, Holmes LB, Atkins L, Riccardi VM: Aniridia-Wilms' tumor association: Evidence for specific deletion of 11p13. *Cytogenet Cell Genet* 1979, 24:185-192
26. Shows TB, Davis LM, Qin S, Nowak NJ: The chromosome 11 gene map: Genes for growth and development, Wilms' tumor deletions, and cancer chromosome break points. *Cold Spring Harbor Symp Quant Biol* 1986, LI:867-877
27. Ngyuen C, Mattei M-G, Mattei J-F, Santoni M-J, Goridis C, Jordan BR: Localization of the human NCAM gene to band q23 of chromosome 11: The third gene coding for a cell molecule mapped to the distal portion of the long arm of chromosome 11. *J Cell Biol* 1986, 102:711-715
28. Morton CC, Byers MG, Nakai H, Bell GI, Shows TB: Human genes for insulin-like growth factors I and II and epidermal growth factor are located on 12q22-q24.1, 11p15, and 4q25-q27, respectively. *Cytogenet Cell Genet* 1986, 41:245-249
29. Reeve AE, Eccles MR, Wilkins RJ, Bell GI, Millow LJ: Expression of insulin-like growth factor-II transcripts in Wilms' tumour. *Nature* 1985, 317:258-260
30. Scott J, Cowell J, Robertson ME, Priestley LM, Wadey R, Hopkins B, Pritchard J, Bell GI, Rall LB, Graham CF, Knott TJ: Insulin-like growth factor-II gene expression in Wilms' tumour and embryonic tissues. *Nature* 1985, 317:260-262
31. Zimmerman KA, Wancopoulos GD, Collum RG, Smith RK, Kohl NE, Denis KA, Nau MM, Witte ON, Toran-Allerand D, Gee CE, Minna JD, Alt FW: Differential expression of myc family genes during murine development. *Nature* 1986, 319:780-783
32. Alt FW, DePinho R, Zimmerman KA, Legouy E, Hatton K, Ferrier P, Tesfaye A, Yancopoulos G, Nisen P: The human myc gene family. *Cold Spring Harbor Symp Quant Biol* 1986, LI:931-941
33. Nisen PD, Zimmerman KA, Cotter SV, Gilbert F, Alt FW: Enhanced expression of the N-myc gene in Wilms' tumors. *Cancer Res* 1986, 46:6217-6222

Acknowledgment

The authors thank Marlis Kasper, Ursula Schaub, and Daniel Wey for skilfull technical assistance, and Drs. Sinika Pelkonen and Christoph Weisgerber for the gift of bacteriophage endosialidase.